Applied Catalysis A: General 467 (2013) 342–354

Contents lists available at ScienceDirect

Applied Catalysis A: General

journal homepage: www.elsevier.com/locate/apcata

Activation of H_2O_2 and superoxide production using a novel cobalt complex based on a polyampholyte

Lucía V. Lombardo Lupano[a], Juan Manuel Lázaro Martínez[b,c], Lidia Leonor Piehl[d], Emilio Rubin de Celis[d], Viviana Campo Dall' Orto[a,e,*]

[a] IQUIFIB-CONICET, Junín 956 (C1113AAD), Ciudad Autónoma de Buenos Aires, Argentina
[b] Departamento de Química Orgánica, Facultad de Farmacia y Bioquímica, Universidad de Buenos Aires, Junín 956 (C1113AAD), Ciudad Autónoma de Buenos Aires, Argentina
[c] IFEG-CONICET, Medina Allende s/n (5000), Córdoba, Argentina
[d] Departamento de Fisicomatemática, Facultad de Farmacia y Bioquímica, Universidad de Buenos Aires, Junín 956 (C1113AAD), Ciudad Autónoma de Buenos Aires, Argentina
[e] Departamento de Química Analítica y Fisicoquímica, Facultad de Farmacia y Bioquímica, Universidad de Buenos Aires, Junín 956 (C1113AAD), Ciudad Autónoma de Buenos Aires, Argentina

ARTICLE INFO

Article history:
Received 7 July 2013
Accepted 1 August 2013
Available online xxx

Keywords:
Heterogeneous catalysis
Cobalt complexes
Polyampholytes
Solid-state NMR
Hydrogen peroxide

ABSTRACT

A new catalyst based on Co(II) and a hydrogel with property of polyampholyte was characterized by equilibrium studies of Co(II) uptake, solid-state NMR and energy dispersive X-ray analysis. The matrix derived from methacrylic acid and 2-methylimidazole is easily synthesized in one-spot strategy, and combines coordination properties with chemical resistance. The catalytic activity of this material on H_2O_2 activation was studied by electron spin resonance, which confirmed the release of superoxide radical. A possible mechanism of interaction involves the simultaneous production of dioxygen, protons and water. The catalytic performance was assessed in the activation of H_2O_2 for the oxidation of two representative organic compounds of environmental concern. About 70% of methyl orange, a model azo dye, was removed from distilled water in 2 h by oxidation with H_2O_2 60 mM and by adsorption on the catalyst. The amount of adsorbed dye was minimized in the presence of 0.1 M Na_2SO_4. The kinetics of the processes followed a pseudo-first-order empirical model, and the catalyst was recovered and re-used. Epinephrine was chosen as a pharmaceutical model susceptible to superoxide attack. About 80% of conversion to adrenochrome was reached in less than 6 min, following a pseudo-first-order kinetic model.

1. Introduction

The advanced oxidation processes using reactive radicals are recognized as effective ways for the degradation of organic pollutants dissolved in water.

Hydrogen peroxide (H_2O_2) is an attractive reagent in detoxification of water polluted with chemicals such as pesticides, phenols, hydrocarbons, surfactants, and dyes. The low environmental impact of this peroxide is based on the fact that water is the only by-product. However it is a rather slow oxidizing agent in the absence of activators [1,2].

In this regard, many different transition metal complexes have been introduced as catalysts due to their ability to activate oxidants. The oxygen radicals from H_2O_2 are efficiently generated only after proper chelation of the cation involved in the catalytic mechanism.

Abbreviations: AICc, Akaike information criterion; C_e, ion concentration at equilibrium; CP-MAS, cross-polarization and magic angle spinning; CW ESR, continuous wave electron spin resonance; DMPO, 5,5-dimethyl-1-pyrroline-N oxide; D–R, Dubinin–Radushkevich; ε, Polanyi potential; E, mean free energy of sorption (D–R); E°, standard reduction potential; EDS, energy dispersive X-ray spectroscopy; K_F, Freundlich sorption constant; MO, methyl orange; pI, isoelectric point; Poly(EGDE-MAA-2MI), polyampholyte derived from ethylene glycol diglycidyl ether methacrylic acid and 2-methylimidazole; q_e, adsorption capacity in equilibrium; q_m, maximum amount of adsorbate that can be adsorbed in micropores (DR); SEM, scanning electron microscopy; R^2, regression coefficient; SOD, superoxide dismutase; TR-XRF, X-ray fluorescence with total reflection; ζ, zeta potential.

* Corresponding author at: Departamento de Química Analítica y Fisicoquímica, Facultad de Farmacia y Bioquímica, Universidad de Buenos Aires, Junín 956 (C1113AAD), Ciudad Autónoma de Buenos Aires, Argentina. Tel.: +54 1149648263; fax: +54 1149648263.
E-mail addresses: vcdall@ffyb.uba.ar, vcdall@yahoo.com.ar (V. Campo Dall' Orto).

0926-860X/$ – see front matter © 2013 Elsevier B.V. All rights reserved.
http://dx.doi.org/10.1016/j.apcata.2013.08.002

The application of the transition metal cobalt in organic transformation has attracted increasing interest especially due to its lower cost when compared with its higher homologues [3].

Cobalt (II) appears to be a good oxygen transfer agent in oxidizing olefins. Reversible redox cycle between Co(II)–Co(III) oxidation states causes oxygen atom transfer to the double bonds by cobalt complexes [4–6].

Besides, the combination of a transition metal with a hydrogel as ligand for heterogeneous catalysis is an interesting approach which facilitates the recovery, regeneration and recycling of the catalyst. In this way, the material can be used in continuous processing, overcoming secondary pollution.

In spite of the good performance of Co(II) catalysts, only a limited number of complexes with polymeric non-soluble supports have been presented.

Cobalt complexes with modified crosslinked polyacrylamide have been reported to be efficient heterogeneous catalysts for selective oxidation of olefins and alkyl halides with H_2O_2 in aqueous media [7].

Cobalt-phtallocyanines immobilized on activated carbon fibres have been used as activators of H_2O_2 on the oxidative removal of 4-nitrophenol [8].

In this work we tested the synthetic polyampholyte Poly(EGDE-MAA-2MI) as ligand for Co(II). The particular relevance of this material is that it combines the benefits of synthetic polymers, i.e. the high adsorption capacity, chemical stability, low costs and simplicity of the synthetic procedure. This polyampholyte is synthesized in a one-step procedure and bears carboxylic and 2-methylimidazole residues, which endows it coordination capacity [9–12].

Here, we studied the catalytic activity of this coordination complex on H_2O_2 activation. The polyampholyte has already been successfully applied on the development of a catalyst based on Cu(II) for the activation of this oxidant [13]. Nevertheless, the Co(II)-derived catalyst was expected to activate H_2O_2 by means of a different mechanism.

In order to explore the applicability of the Co(II)-Poly(EGDE-MAA-2MI)catalyst in the environmental and industrial fields, we chose two different types of organic substrates: methyl orange (a model compound of synthetic dyes), and epinephrine (a model compound of pharmaceuticals).

Methyl orange (MO) is used as pH indicator in 0.1% aqueous solution, as well as in dyeing and printing textiles. It is considered a hazardous substance according to OSHA 29 CFR 1910.1200. It is chemically stable and both, its persistence in water and soil and its mobility are high [14].

The degradation products of MO by the action of highly reactive oxygen-containing species are well described. The photo-Fenton degradation of MO produces 4-dimethylamino aniline, suggesting an N—N bond cleavage of the azo linkage [15]. The hydroxylated and non-hydroxylated species have been identified by Baiocchi et al. [16] and He et al. [17].

Parshetti et al. studied the phytotoxicity and microbial toxicity of the dye and some degradation products [18] and found that MO is toxic and that the metabolites obtained, such as 4-amino sulfonic acid and *N*,*N*-dimethyl p-phenyldiamine, are nontoxic for experimental plants (*Triticum aestivum* and *Phaseolus mungo*) and bacteria (*Kocuria rosea*, *Pseudomonas aurugenosa* and *Azatobacter vinelandii*).

Epinephrine is a catecholamine, susceptible to peroxide attack. It can be partially oxidized by superoxide to the industrial product adrenochrome (catecholamine *o*-quinone), a precursor of haemostatic drugs such as carbazochrome [19,20].

2. Experimental

2.1. Materials and reagents

2-Methylimidazole (2MI; 99 wt%), methacrylic acid (MAA; 99 wt%), ethylene glycol diglycidyl ether (EGDE; 50 wt% in ethylene glycol dimethylether), epinephrine bitartrate and 5,5-dimethyl-1-pyrroline-N oxide (DMPO) were purchased from Sigma–Aldrich. Benzoyl peroxide was purchased from Fluka. Superoxide dismutase (SOD) was purchased from Biosidus (Buenos Aires, Argentina). Acetonitrile from Baxter was of HPLC grade.

$CoSO_4$ and cobalt acetate were purchased from Mallincrodt (USA). Na_2SO_4 and H_2O_2 (30 wt%) were acquired from Merck (Darmstadt, Germany). Methyl Orange was from Santa Cruz Biotechnology, Inc.

Water was distilled with a FIGMAY glass apparatus (Córdoba, Argentina). All other reagents were of analytical grade.

2.2. Instruments

High-resolution ^{13}C solid-state spectra for the polymers were recorded using the ramp $\{^1H\} \rightarrow \{^{13}C\}$ CP-MAS (cross-polarization and magic angle spinning) sequence with proton decoupling during acquisition. All the solid-state NMR experiments were performed at room temperature in a Bruker Avance II-300 spectrometer equipped with a 4-mm MAS probe. The operating frequency for protons and carbons was 300.13 and 75.46 MHz, respectively. Glycine was used as an external reference for the ^{13}C spectra and to set the Hartmann–Hahn matching condition in the cross-polarization experiments. The recycling time was 4 s. Two different contact times during CP were employed: 800 and 1500 μs. The SPINAL64 sequence was used for heteronuclear decoupling during acquisition with a proton decoupling field H_{1H} satisfying $\omega_{1H}/2\pi = \gamma_H H_{1H} = 62$ kHz [21]. The spinning rate for all the samples was 10 kHz.

The surface of the polymers was characterized using scanning electron microscopy (SEM) and the elemental composition of cobalt and sulfur in different parts of the materials was performed by energy dispersive X-ray spectroscopy (EDS). SEM imaging and EDS were carried out with a scanning electron microscope Field Emission SEM (Zeiss Gemini DSM 982) operated at a 0.3 kV acceleration voltage and an INCA Energy (Oxford Instrument), respectively.

The electron spin resonance (ESR) spectra were obtained at 20 °C using an X-band ESR Spectrometer Bruker EMX plus (Bruker Instruments, Inc., Berlin, Germany).

Partial pressure of dioxygen was measured with an Orbisphere A1100 – Oxygen Sensor.

UV–visible spectrophotometric measurements were made on a Hewlett-Packard instrument, HP 8452A model with diode array.

Cobalt ions released from the complex to the solution were analysed with a BRUKER X-ray fluorescence spectrometer with geometry of total reflection (TR-XRF), PICOFOX S2 model.

2.3. Cobalt uptake

Cobalt binding studies were performed with 0.0500 g of polyampholyte and 4.0 mL of $CoSO_4$ solution in a 2.6–21 mM concentration range. The samples were centrifuged and filtered after 48 h of contact time at 24 °C. Free Co(II) concentration at the equilibrium in each supernatant solution could be determined spectrophotometrically since Co^{2+} forms a coordination compound with SCN^- in presence of HCl and acetone, which absorbs radiation at 622 nm [22].

2.4. Model fitting by non-linear regression

The isotherm and kinetic parameter sets were determined by non-linear regression. The algorithm based on the Gauss–Newton method was used. The error function employed to evaluate the fit was the second order corrected Akaike information criterion (AIC_C) [23]. The Akaike weights provide information about the strengths of evidence supporting the two competing models. The evidence ratio rising from the Akaike criterion represents the relative likelihood favouring the better of two competing models. As reported by other authors, an evidence ratio greater than 20, would indicate extremely strong evidence favouring the better model [24,25].

2.5. Co(II)-Poly(EGDE-MAA-2MI) complex preparation

The complex was prepared mixing 0.5000 g of polyampholyte powder and 40 mL of 70 mM $CoSO_4$ solution in distilled water at 24 °C for 48 h. The samples were then centrifuged, washed with three 20-mL portions of distilled water to remove the Co(II) weakly adsorbed on the particles, filtered, dried at 60 °C and milled in a mortar. It must be mentioned that the last portion of water from the wash step did not present detectable amounts of free Co(II) in solution, when it was tested by the colorimetric method described in Section 2.3.

2.6. Measurement of H_2O_2 concentration

This peroxide reacts with phenol and 4-aminoantipyrine in presence of soybean peroxidase, giving a product that absorbs radiation at 505 nm [26]. The absorbance of the mixture is proportional to the concentration of H_2O_2 when this peroxide is the reagent in defect. The reaction is presented in Scheme A.1 (Supplementary content).

In this way, a solution of the 4-aminoantipyrine reagent was prepared with 9 mg of 4-aminoantipyrine, 200 mg of phenol and 0.1 M phosphate buffer at pH 7.0 to a final volume of 10 mL.

An amount of 0.0500 g of Co(II)-Poly(EGDE-MAA-2MI) was suspended in 50 mL of 42 mM H_2O_2 and 0.1 M Na_2SO_4 solution. The concentration of H_2O_2 was monitored as a function of time from 20-μL samples of the reaction, which were mixed with 60 μL of 300 U mL^{-1} of soybean peroxidase extract, 100 μL of the solution of 4-aminoantipyrine reagent and 480 μL of 0.1 M phosphate buffer at pH 7.0 [26].

The salt, Na_2SO_4, was added to most of the solutions in order to minimize the adsorption of organic compounds on the surface of the catalyst.

2.7. Measurement of free radicals by ESR

The initial H_2O_2 concentration was set close to 60 mM. Higher concentration levels of H_2O_2 were expected to be less efficient in oxidative processes due to possible deleterious effect on the polymeric catalyst [13].

An amount of 0.0500 g of Co(II)-Poly(EGDE-MAA-2MI) was suspended in 50 mL of 63 mM H_2O_2 solution and the production of free radicals was followed by ESR. The medium of reaction was alternatively distilled water or 0.1 M Na_2SO_4 solution.

For a control experiment, we used a Co(II)-Poly(EGDE-MAA-2MI) complex obtained from cobalt acetate instead of the original Co(II)-Poly(EGDE-MAA-2MI) complex obtained from $CoSO_4$.

The experiment was also performed in presence of SOD with an activity of 200 U mL^{-1}, added to the system before of H_2O_2.

Aliquots of 32 μL taken at different times of reaction were mixed with 16 μL of 3 M DMPO (spin trap), and the continuous wave (CW) ESR spectra of the DMPO spin adducts were recorded at 20 °C 3 min after the end of incubation.

The spectrometer settings were: centre field: 3515 G, sweep width: 100 G, microwave power: 10 mW, microwave frequency: 9.85 GHz, conversion time: 2.56 ms, time constant: 2.56 ms, modulation frequency: 50 KHz, modulation amplitude: 0.11 G, gain: 2.00×10^4, resolution: 1024 points. All spectra were the accumulation of 20 scans. DMPO adduct signal intensities were measured as the total height of the first field peak in the respective ESR spectra.

The ESR spectra were simulated by means of an Electron Spin Resonance Simulator using for the fitting the Levenberg–Marquardt algorithm. Molar proportion yields and hyperfine interaction constant values were calculated from the simulated spectra.

2.8. Methyl orange decolorization

An amount of 0.1000 g of Co(II)-Poly(EGDE-MAA-2MI) was suspended in 100 mL of 41 ± 1 μM MO and 63 mM H_2O_2 solution. The medium of reaction was alternatively distilled water or 0.1 M Na_2SO_4 solution. The absorbance of the solution was monitored as a function of time at 464 nm. For turbidity correction, the absorbance was measured at 700 nm and subtracted to the absorbance at 464 nm.

The control of MO adsorption on the catalyst was made in absence of H_2O_2.

The control of H_2O_2 activation in homogeneous phase was made with a 0.35 mM $CoSO_4$ solution, 41 μM MO, 63 mM H_2O_2 and 0.1 M Na_2SO_4. This control was made to determine if any free and soluble Co(II) species could interact with H_2O_2 and generate free radicals in solution.

For the evaluation of the chemical stability of the catalyst on reutilization, the experiment of MO decolorization was repeated three times with the same recycled catalyst and new aliquots of solution. Each cycle had an extension of 30 min, and was carried out in 0.1 M Na_2SO_4 solution. After each catalytic cycle, the suspension was centrifuged, the supernatant was discarded, the solid was washed twice with 0.1 M Na_2SO_4 and with a portion of distilled water, and then it was dried at 40 °C for a new use.

In order to explore the regeneration of the catalyst used for the first catalytic cycle, the solid was recovered by centrifugation, washed with three portions of distilled water and dried at 40 °C. Then 0.1000 g of the used catalyst were reloaded with 8 mL of 70 mM $CoSO_4$ solution in distilled water at 24 °C for 24 h. The mixture was centrifuged, washed with three 20-mL portions of distilled water to remove the Co(II) weakly adsorbed on the particles, filtered, dried at 40 °C and milled in a mortar to be used in a new catalytic cycle.

Another control dealt with the chemical stability of the MO molecules adsorbed on the particles. An aliquot of 0.2000 g of Co(II)-Poly(EGDE-MAA-2MI) was suspended in 200 mL of 41 ± 1 μM MO solution in 0.1 M Na_2SO_4, the suspension was centrifuged, the solid was washed with three portions of distilled water and dried at 40 °C. An amount of 0.1000 g of the MO-loaded Co(II)-Poly(EGDE-MAA-2MI) was put in contact with 100 mL of a 63 mM H_2O_2 solution in 0.1 M Na_2SO_4, which had been previously activated with the catalyst during 10 min. The experiment was repeated with another 0.1000-g aliquot of the MO-loaded Co(II)-Poly(EGDE-MAA-2MI) and the 63 mM H_2O_2 solution in 0.1 M Na_2SO_4 without previous activation. In both cases, we looked for a decrease of the colour intensity of the particles.

For the detection of cobalt intermediate species catalytically active, 0.1000 g of Co(II)-Poly(EGDE-MAA-2MI) were put in contact with 100 mL of 63 mM H_2O_2 and 0.1 M Na_2SO_4 solution during 10 min. The suspension was centrifuged, the supernatant was discarded, the particles were washed with three portions of distilled water, and they were not dried. The activated particles of the catalyst were put in contact with 100 mL of 41 ± 1 μM MO solution in 0.1 M Na_2SO_4 and the MO concentration was monitored as a

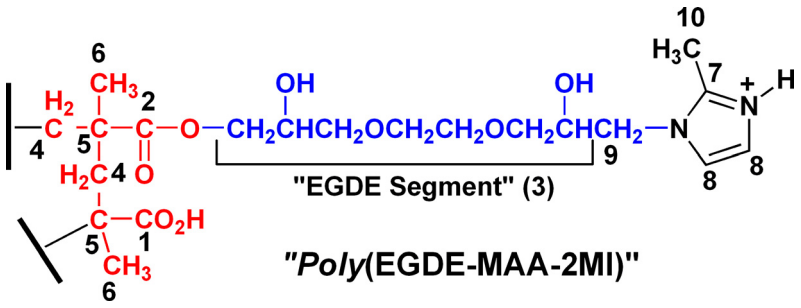

Scheme 1. Representative chemical structure of Poly(EGDE-MAA-2MI).

function of time by visible spectrophotometry. The activation of the solid with H_2O_2 was repeated twice, and the catalyst was put in contact with the same MO solution after each activation cycle in order to monitor the concentration of the dye.

2.9. Epinephrine oxidation

An amount of 0.0400 g of Co(II)-Poly(EGDE-MAA-2MI) was suspended in 20 mL of 2 mM epinephrine and 46 mM H_2O_2 solution (higher concentrations of H_2O_2 were proved to be less effective). The medium of reaction was 0.1 M Na_2SO_4 solution. The absorbance of the solution was monitored as a function of time at 480 nm. For turbidity correction, the absorbance was measured at 700 nm and subtracted to the absorbance at 480 nm.

A control experiment of epinephrine oxidation in homogeneous system was made with a solution of 2 mM epinephrine and 46 mM H_2O_2 in 0.1 M Na_2SO_4.

Another control experiment was made with 0.0400 g of Co(II)-Poly(EGDE-MAA-2MI) suspended in 20 mL of 2 mM epinephrine and 0.1 M Na_2SO_4, in absence of H_2O_2. This experiment was repeated with previous and continuous bubbling of argon in the epinephrine solution, in order to displace the dissolved O_2.

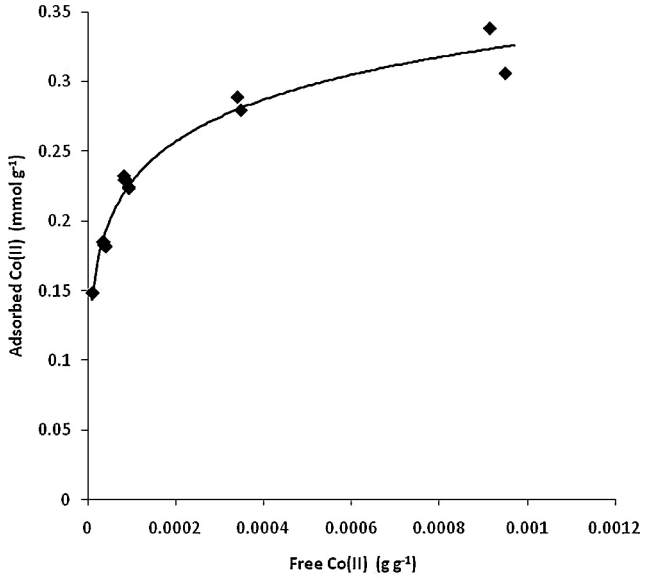

Fig. 1. Adsorption isotherm of Co(II) onto the polyampholyte at 24 °C. Experimental data fitted to the D–R model.

3. Results and discussion

3.1. Synthesis and characterization of the polyampholyte

The material was synthesized via reaction of the selected monomers in the presence of benzoyl peroxide. Scheme 1 shows the representative chemical structure for Poly(EGDE-MAA-2MI).

The mechanism of synthesis and the chemical structure of this material have been studied by means of a variety of spectroscopic methods, and carefully described in previous reports [9–12]. Here, we present the characterization of the polyampholyte production batch used for these experiments [25].

The material is synthesized as a monolith, and then milled into particles. The isoelectric point (pI) for this material determined by the measurements of ζ (zeta potential) was 6.77. The apparent diameter of the particles was 64 ± 4 μm [27].

These particles have 0.89 mmol g^{-1} of titrable carboxylate and 1.09 mmol g^{-1} of titrable 2MI residues, besides the hydroxyl groups (Scheme 1). The pI calculated from the titrable functional groups (6.75) coincided with the value obtained from the ζ measurements.

3.2. Cobalt adsorption equilibrium

The mechanism of cobalt uptake was explored analysing the results of the adsorption isotherm for the polyampholyte at 24 °C. Four isotherm models (Langmuir, Dubinin–Radushkevich (D–R), Freundlich and Temkin) were used to fit the experimental adsorption data by non-linear regression.

The best fit of experimental adsorption data was obtained with the D–R (Fig. 1), Temkin and Freundlich isotherms (Supplementary content, Fig. A.1), according with the evidence ratio based on the Akaike criterion [25]. The Langmuir model had no statistical support due to its significantly larger residual sum of squares.

The Freundlich model can be described as:

$$q_e = K_F(C_e^{1/n}) \quad (1)$$

where q_e is the adsorption capacity in equilibrium with the corresponding C_e (mmol L^{-1}), which is the concentration of metal ion.

This model assumes that the surface is heterogeneous in the sense that the adsorption energy is distributed and the surface topography is patchwise [28]. The sites with the same adsorption energy are grouped together into one patch (the adsorption energy here is the energy of interaction between adsorbate and adsorbent). Each patch is independent of each other (i.e., there is no interaction between patches) and the Langmuir equation is applicable for the description of equilibrium of each patch.

K_F can be defined as the sorption or distribution coefficient and represents the amount of Co(II) sorbed onto the polymer surface normalized by the equilibrium concentration and $1/n$ is a measure of surface heterogeneity, ranging between zero and one which becomes more heterogeneous as its value gets closer to zero [29].

Table 1
Isotherm parameters for Co(II) adsorption on the polyampholyte. Regression coefficients (R^2), values of AIC_C criterium and evidence ratio for Freundlich, Temkin, Dubinin–Radushkevich (D–R) and Langmuir models.

Freundlich		Temkin		Dubinin–Radushkevich		Langmuir	
n	5.87 S.D.: 0.30	b_T (kJ mol^{-1})	61.1S.D.: 2.8	q_m (mmol g^{-1})	0.521 S.D.: 0.018	q_m, (mmol g^{-1})	0.298S.D.: 0.013
K_F (mmol g^{-1})	0.2059S.D.: 0.0031	K_T (mmol L^{-1})	181 S.D.: 48	B (mol^2 kJ^{-2})	1.60×10^{-3}S.D.:7×10^{-5}	K_L	0.332S.D.: 0.067
				E (kJ mol^{-1})	17.68 S.D.: 0.39		
R^2	0.9666	R^2	0.9731	R^2	0.9754	R^2	0.815
AIC_C	−133.0	AIC_C	−134.6	AIC_C	−137.4	AIC_C	−107.3
Evidence ratio	8.6	Evidence ratio	4.0	Evidence ratio	1	Evidence ratio	3.2×10^6

The Temkin model assumes that the heat of adsorption (which is a function of temperature) of all molecules in the layer will decrease linearly rather than logarithmically with coverage [30].

$$q_e = \frac{RT}{b_T} \ln(K_T C_e) \quad (2)$$

The Dubinin–Radushkevich isotherm is a semi-empirical equation which was originally developed for sub-critical vapours in microporous solids, where the adsorption process follows a pore-filling mechanism:

$$q_e = q_m e^{-B_D \varepsilon^2} \quad (3)$$

where q_m is the maximum amount of adsorbate that can be adsorbed in micropores, and B_D is a constant related to the energy.

The value estimated for q_m was 30.7 mg of Co(II) per gram of polyampholyte, significantly higher than that predicted by Langmuir model (17.6 mg g^{-1}), summarized in Table 1. This loading capacity for Co(II) was lower than the capacity for Cu(II), estimated in 0.90 mmol or 57 mg g^{-1} [10].

Liquid-phase adsorption data can also be analysed by the equation below, where the amount adsorbed corresponding to any adsorbate concentration is assumed to be a Gaussian function of the Polanyi potential (ε),

$$\varepsilon = RT \ln\left(1 + \frac{1}{C_e}\right). \quad (4)$$

R, T and C_e represent the gas constant (8.314×10^{-3} kJ mol^{-1} K^{-1}), absolute temperature (K), and ion concentration at equilibrium (g ion per gram of solution), respectively [31].

The equation is generally applied to express the adsorption mechanism with a Gaussian energy distribution onto a heterogeneous surface. The approach is usually applied to distinguish the physical and chemical adsorption of metal ions by means of the equation

$$E = \frac{1}{\sqrt{2B_D}}. \quad (5)$$

The parameter E is the mean free energy of sorption [32], whose magnitude is a way to estimate the type of sorption process.

In the case E is lower than 8 kJ mol^{-1}, weak physical forces, such as van der Waals and hydrogen bonding, may affect the sorption mechanism. If this value is between 8 and 16 kJ mol^{-1}, the sorption process can be explained by ion exchange. If this value is higher than 16 kJ mol^{-1}, the sorption process can be explained by other chemical reactions such as coordination [33].

The E value and other parameters calculated for all the models tested are summarized in Table 1. The E value higher than 16 kJ mol^{-1} K^{-1} suggests the coordination of Co(II) with the —OH, —COO$^-$ and/or 2MI residues of the polyampholyte. The deep violet colour of the particles of Co(II)-poly(EGDE-MAA-2MI) is another evidence of coordination (Fig. 2).

For further experiments, we prepared a Co(II)-Poly(EGDE-MAA-2MI) complex with a load of 30.7 mg Co(II) per gram estimated from the isotherm fit.

3.3. SEM and EDS analysis

Co(II)-Poly(EGDE-MAA-2MI) was characterized using SEM in order to evidence surface morphological changes when compared with the polyampholyte. The SEM images are depicted in Fig. 3A and B. The surface of Co(II)-Poly(EGDE-MAA-2MI) exhibited a significant difference in homogeneity degree. The image also suggests a small increase in surface area.

The identity of Co^{2+} counterion was manifested in EDS (Fig. 3C–E). The sulfur in the sample was present when $CoSO_4$ was used to obtain the complex and absent in complexes derived from cobalt acetate. The presence of SO_4^{2-} evidences the existence of fixed positive charges on the surface of the particles, coming from the Co(II) and/or NH^+ from the 2MI residues. SO_4^{2-} could eventually be exchanged by other anions, as discussed below.

3.4. Solid-state NMR analysis

Solid-state NMR spectroscopy was used to characterize the Co(II)-complexes to obtain an approximation of the ligands involved in the coordination sphere of the metal ion in the polymer matrix, since the paramagnetic ions produce a strong source of relaxation. In particular, we have previously observed that the carbon signal of the carboxylic acid in the ^{13}C CP-MAS is a sensitive parameter to sense the union of the paramagnetic Cu^{2+} ion to this ligand (RCO_2H) [11].

The ^{13}C CP-MAS spectra for the Poly(EGDE-MAA-2MI) polymer and its cobaltous complexes with 8.7 and 30.7 mg of Co^{2+} per gram of polymer material are shown in Fig. 4. The most significant changes were observed with the highest amount of adsorbed Co^{2+}, where the signals of the carbons from the imidazole ring (C_{7-8}) and the carboxylic acid (C_1) were completely depleted in the ^{13}C CP-MAS spectra. This behaviour indicates that the paramagnetic centres of Co^{2+} strongly interacted with these ligands, leading to the broadening and disappearance of the resonance signals at 30.7 mg of Co^{2+} per gram of polymer. For that reason, the contact time with the cross-polarization, in the ^{13}C CP-MAS experiments, was reduced to 800 μs, in comparison with the 1500 μs used in the other ^{13}C CP-MAS spectra. Additionally, since the polymer matrix did not present positive permanent domains (i.e. absence

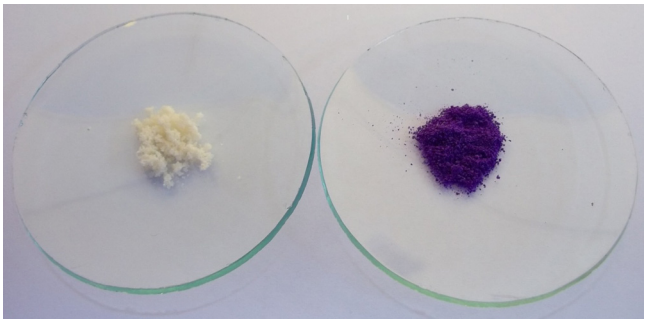

Fig. 2. Picture of Poly(EGDE-MAA-2MI) (left) and Co(II)-Poly(EGDE-MAA-2MI) (right).

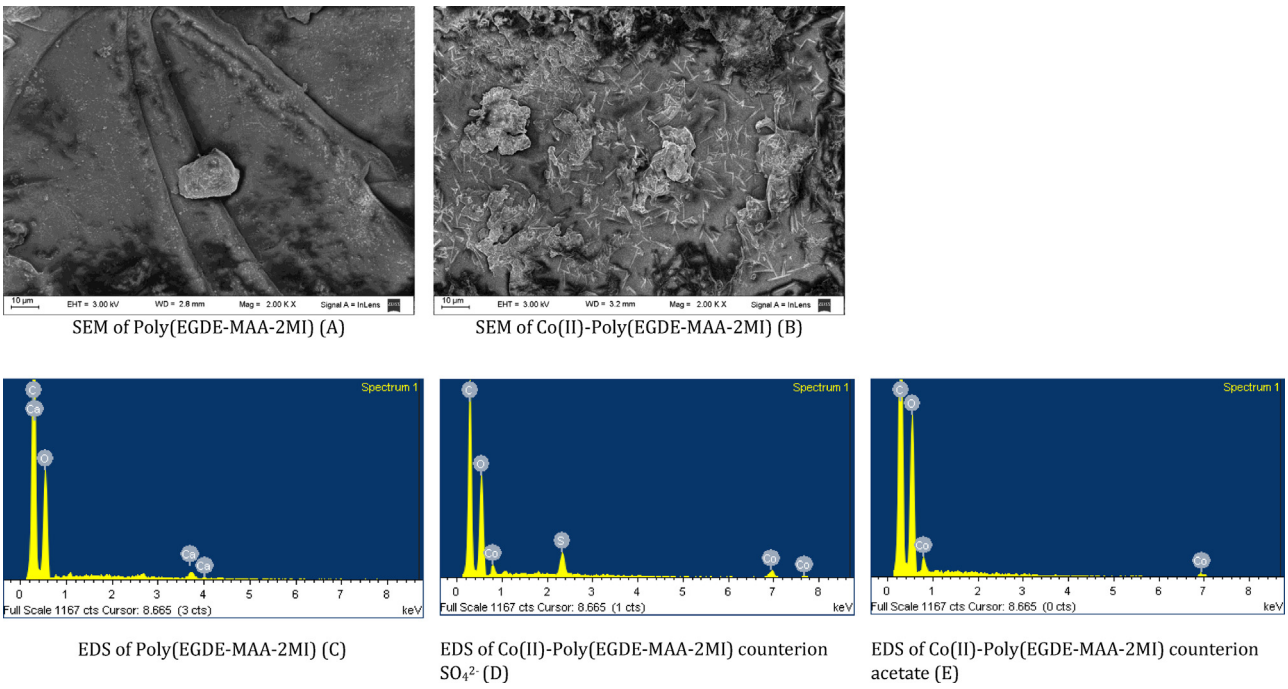

Fig. 3. SEM images for the surface of Poly(EGDE-MAA-2MI) (A) and Co(II)-Poly(EGDE-MAA-2MI) (B) at a magnification of 2K×. EDS spectra of Poly(EGDE-MAA-2MI) (C), Co(II)-Poly(EGDE-MAA-2MI) obtained from $CoSO_4$ (D) and Co(II)-Poly(EGDE-MAA-2MI) obtained from cobalt acetate (E).

of N_1,N_3-disubstitution of the imidazole moieties), as determined from the potentiometric titration and zeta-potential measures, we observed a complete reduction of the imidazole signals, making a difference with a Cu(II)-complex where the polymer matrix contains 45% of N_1,N_3-disubstitution of the imidazole units [11]. At low levels of adsorbed cobaltous ion (8.7 mg Co^{2+} g^{-1}), the effect of the ion was slightly observed in the intensity of the signals of C_9 and C_{10}. Although this change might be attributed to modifications in the reticulation of the materials, the signals of the ligands were not perturbed (C_{1-7-8}). That made a difference with some Cu(II)-complexes where the signal of C_1 was specially affected with 8 mg of copper per gram of polymer [11], having into account that the Cu^{2+} ions have a higher reduction effect in the relaxation times of ^1H than Co^{2+} ions [34]. With these results, the cobaltous ions might be coordinated with the oxygens of the carboxylic acid and the nitrogens of the imidazole moieties at 30.7 mg of Co^{2+} per gram of polymer.

Scheme 2 shows the possible chemicals structures of the Co(II)-Poly(EGDE-MAA-2MI) complexes. The most probable geometries are square-planar and octahedral, with the cobaltous ion coordinated by different combinations of —COO^- and 2MI groups.

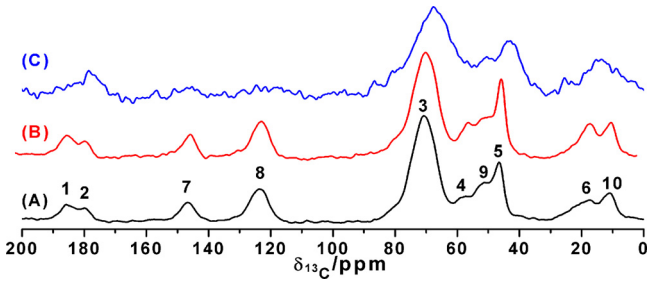

Fig. 4. ^{13}C CP-MAS spectra for Poly(EGDE-MAA-2MI) (A) and for its Co(II)-complexes containing 8.7 (B) and 30.7 mg of Co^{2+} per gram of polymer (C). The numbering corresponds to that in Scheme 1.

3.5. H_2O_2 activation

We have previously demonstrated that Poly(EGDE-MAA-2MI) has no catalytic activity on H_2O_2 activation [13]. Now, the Co(II)-Poly(EGDE-MAA-2MI) complex was put in contact with 42 mM H_2O_2 in 0.1 M Na_2SO_4, and the concentration of H_2O_2 was monitored as a function of time (Supplementary content, Fig. A.2). The reaction followed a pseudo-first-order kinetics, in agreement with the evidence ratio based on the Akaike criterion:

$$[H_2O_2]_t = [H_2O_2]_\infty + [H_2O_2]_{deg} \times e^{-k \times t} \quad (6)$$

with 37.53 mM $[H_2O_2]_\infty$ (S.D.: 0.30), 4.63 mM $[H_2O_2]_{deg}$ (S.D.: 0.45) and 0.076 min^{-1} k (S.D.: 0.018); R^2 was 0.9642.

A fast decrease of H_2O_2 concentration was observed during the first 20 min of reaction, followed by an asymptotic approach to 37.53 mM.

When the initial amount of H_2O_2 was increased to 63 mM, the changes of concentration as a function of time were less significant due to the large excess of this oxidant. Nevertheless, the activation of the peroxide was evidenced by the set of experiments described below.

The appearance of a certain amount of bubbles suggested the formation of dioxygen as a possible product of H_2O_2 activation. The partial pressure of the gas in the system containing the catalyst was measured before and after the addition of H_2O_2. The increase by 66% in the O_2 partial pressure confirmed the formation of molecular oxygen during the first 5 min of the reaction (Supplementary content, Fig. A.3). Besides, the pH decreased from 6.0 to 4.8 during the reaction.

The evolution of gas bubbles from the surface of the particles of Co(II)-Poly(EGDE-MAA-2MI) as a consequence of the addition of H_2O_2 and only in the presence of immobilized Co(II), clearly evidences that the activation of hydrogen peroxide does not involve a homogeneous catalysis.

The production of free radicals that diffuse into the solution was confirmed by spin trapping experiments with DMPO. Fig. 5A shows the CW ESR spectrum produced by aliquots of supernatant from the

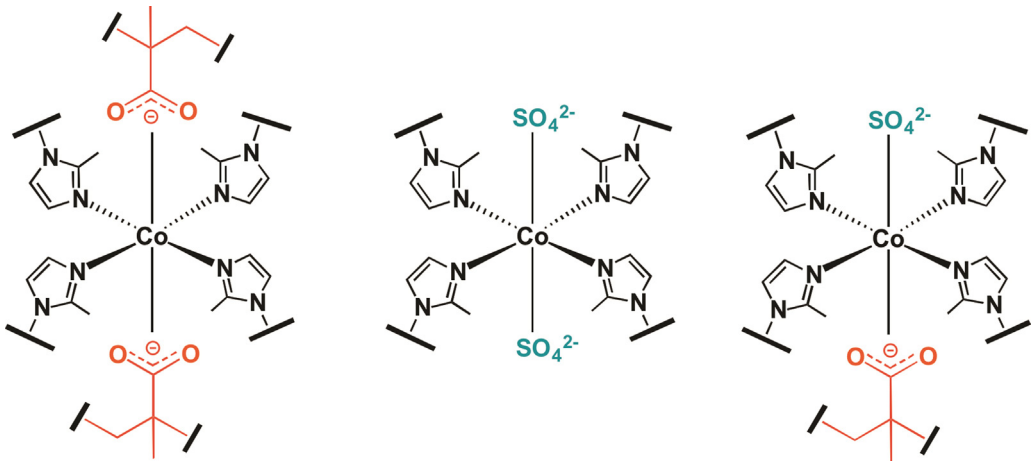

Scheme 2. Most probable geometries of the coordination complex Co(II)-poly(EGDE-MAA-2MI).

Co(II)-Poly(EGDE-MAA-2MI)/63 mM H_2O_2 heterogeneous system, in the presence of DMPO spin trap measured beyond 10 min after the addition of H_2O_2 in 0.1 M Na_2SO_4.

The identity of the free radicals had to be confirmed by additional experiments. According with the profile of the signal, the probable adducts were: DMPO/OSO_3H from $SO_4^{\bullet-}$ [35] and DMPO/OOH from $O_2^{\bullet-}$ [36]. The first option, $SO_4^{\bullet-}$, was considered the least probable due to the expected higher E° of this free radical, when compared with the E° of $OH^{\bullet}$ (+2.8 V vs HNE).

Then, the experiment was repeated in distilled water instead of 0.1 M Na_2SO_4, in order to evaluate the reactivity of SO_4^{2-} ions. The ESR spectrum did not change significantly (Supplementary content, Fig. A.4B) when compared with Fig. 5A. It must be pointed out that the kinetics of the free radical indicated a maximal production at 10 min of reaction (Supplementary content, Fig. A.3), reaching a constant concentration level beyond the 20 min.

However, the $SO_4^{\bullet-}$ species could still arise from the SO_4^{2-} counterions of the positive sites on Co(II)-Poly(EGDE-MAA-2MI) particles. So, the experiment was repeated in distilled water with the Co(II)-poly(EGDE-MAA-2MI) catalyst obtained from cobalt acetate salt instead of $CoSO_4$ (i.e. the absence of sulfur had been confirmed by EDS, Fig. 3E). Again, the same profile in the ESR spectrum was obtained even in the absence of SO_4^{2-}, thus discarding the production of $SO_4^{\bullet-}$ radicals (Supplementary content, Fig. A.5B).

When considering the second option, $O_2^{\bullet-}$, we found that the simulation and fits of the experimental spectrum from Fig. 5A allowed establishing the presence of two species: DMPO/OOH and DMPO/OH adducts from $O_2^{\bullet-}$ and $OH^{\bullet}$, respectively (Fig. 5B) [37].

Table 2
Hyperfine interaction constant values for the DMPO/OOH and the DMPO/OH adducts. The data were obtained by simulation and fits of the experimental spectra.

Radical	a_N (G)	$a_{H\beta}$ (G)	$a_{H\gamma}$ (G)
DMPO/OOH	13.8	11.0	Not resolved
DMPO/OH	14.7	13.8	–

The molar fractions of DMPO/OOH and DMPO/OH adducts were 0.88 and 0.12 respectively.

Fig. 6 shows simulated DMPO/OOH and DMPO/OH adducts separated from each other. The simulated spectrum of Figs. 5B and 6C was obtained by the addition of the above mentioned adducts. It should be noted that the Hγ hyperfine interaction of the DMPO/OOH adduct was not resolved. Table 2 shows the hyperfine interaction constant values for the DMPO/OOH and DMPO/OH adducts.

The presence of the DMPO/OOH adduct was also confirmed by the addition of SOD with an activity of 200 U mL^{-1}. In this case we expected the dismutation of the superoxide radical and the absence of an ESR signal. Instead, we found a spectrum with the characteristic shape of hydroxyl radical adduct.

Fig. 7A shows the CW ESR spectrum obtained when the experiment was performed with the Co(II)-poly(EGDE-MAA-2MI)/63 mM H_2O_2 system in the presence of DMPO and SOD, in distilled water. The simulation (Fig. 7B) and fits of the experimental spectrum allowed establishing the presence of DMPO/OH. The same result

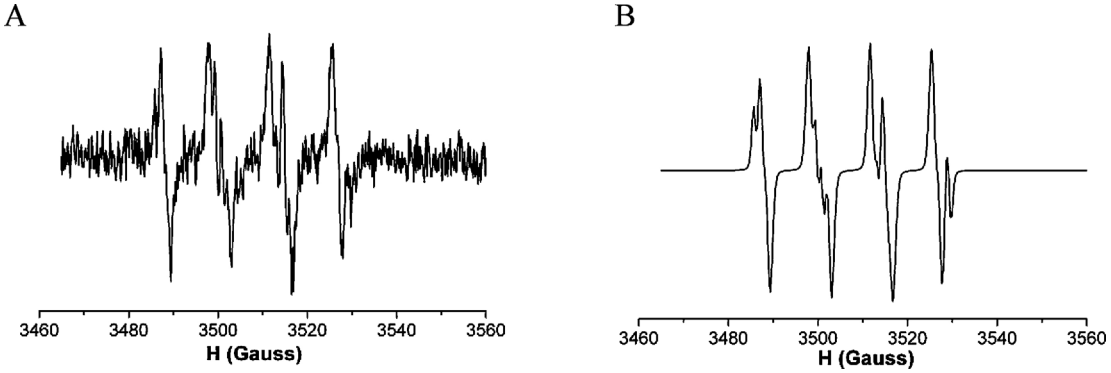

Fig. 5. Experimental (A) and simulated (B) CW ESR in band X spectra from spin trapping experiments with DMPO. Heterogeneous system: Co(II)-Poly(EGDE-MAA-2MI)/63 mM H_2O_2 in 0.1 M Na_2SO_4. The simulation and fits of the experimental spectrum allowed establishing the presence of two species: a DMPO/OOH and a DMPO/OH adducts. The molar fractions of DMPO/OOH and DMPO/OH adducts were 0.88 and 0.12 respectively.

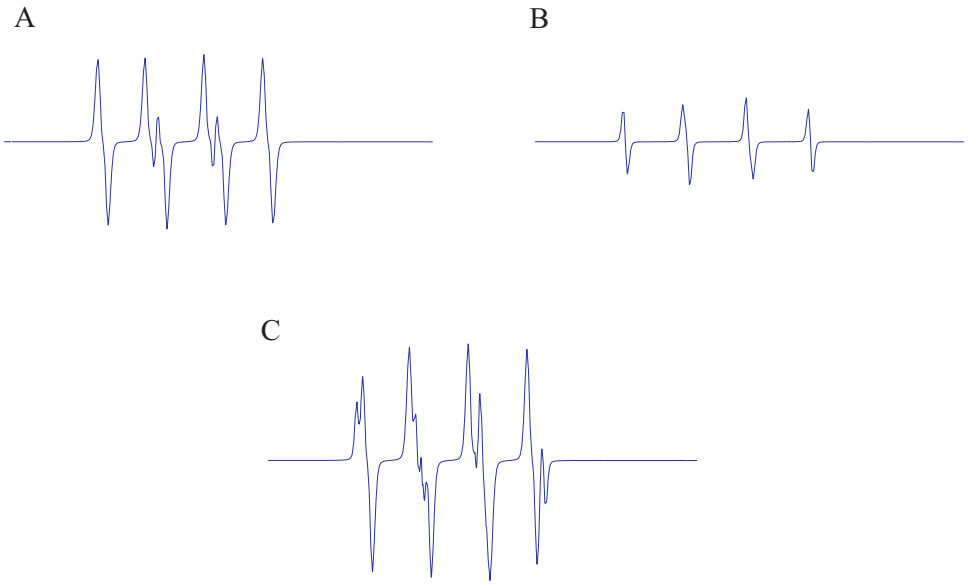

Fig. 6. Simulated DMPO/OOH adduct (A), simulated DMPO/OH adduct (B) and simulated spectrum (C) obtained by the addition of (A) and (B). It should be noted that the Hγ hyperfine interaction of DMPO/OOH adduct was not resolved.

was obtained when the experiment was performed in the presence of SOD in 0.1 M Na_2SO_4 (Supplementary content, Fig. A.6).

Summarizing, the identity of the ESR signal was confirmed: the DMPO/OOH adduct from $O_2^{\bullet -}$ was generated by the Co(II)-poly(EGDE-MAA-2MI)/63 mM H_2O_2 system, and was absent in the presence of SOD due to a fast dismutation of the radical.

Based on this experimental evidence, we propose two mechanisms of H_2O_2 activation catalysed by immobilized Co(II).

The most probable mechanism of activation involves the production of O_2, $O_2^{\bullet -}$ and H^+ according with [36]:

$$\text{L-Co(II)} + 2H_2O_2 \rightleftharpoons \text{L-Co(III)} + 2H_2O + O_2^{\bullet -}$$

$$2\text{L-Co(II)} + H_2O_2 \rightleftharpoons 2\text{L-Co(III)} + O_2 + 2H^+$$

where L-Co(II) represents Co(II)-Poly(EGDE-MAA-2MI).

In order to explain the occurrence of the signal attributed to the DMPO/OH adduct as a minor product of the reaction and as the main product after the addition of SOD, the first step should be split as follows:

$$\text{L-Co(II)} + H_2O_2 \rightleftharpoons \text{L-Co(III)} + OH^- + OH^{\bullet}$$

$$OH^{\bullet} + H_2O_2 \rightleftharpoons HO_2^{\bullet} + H_2O$$

$$HO_2^{\bullet} \rightleftharpoons O_2^{\bullet -} + H^+$$

$$H^+ + OH^- \rightleftharpoons H_2O$$

The stage of $OH^{\bullet}$ degradation must be the slowest in the presence of the enzyme SOD, which would explain the observation of the DMPO/OH signal.

Here we found a significant difference in the mechanism exhibited by a related catalyst, Cu(II)-Poly(EGDE-MAA-2MI). This copper-based material led to the release of $OH^{\bullet}$ species on the activation of H_2O_2 [13]. Besides, the cation suffered a reduction to Cu(I) in the catalytic process [38].

Other speculative mechanism of H_2O_2 activation compatible with the production of O_2 and radicals would be the oxidation of Co(II)-Poly(EGDE-MAA-2MI) by H_2O_2 as follows [39]:

$$\text{L-Co(II)} + 2H_2O_2 \rightleftharpoons HO_2^{\bullet} + OH^{\bullet} + [(H_2O)\text{L-Co(III)}]^+$$

$$HO_2^{\bullet} \rightleftharpoons O_2^{\bullet -} + H^+$$

$$2[(H_2O)\text{L-Co(III)}]^+ + H_2O_2 \rightleftharpoons 2\text{L-Co(II)} + H_2O + O_2 + 2H^+$$

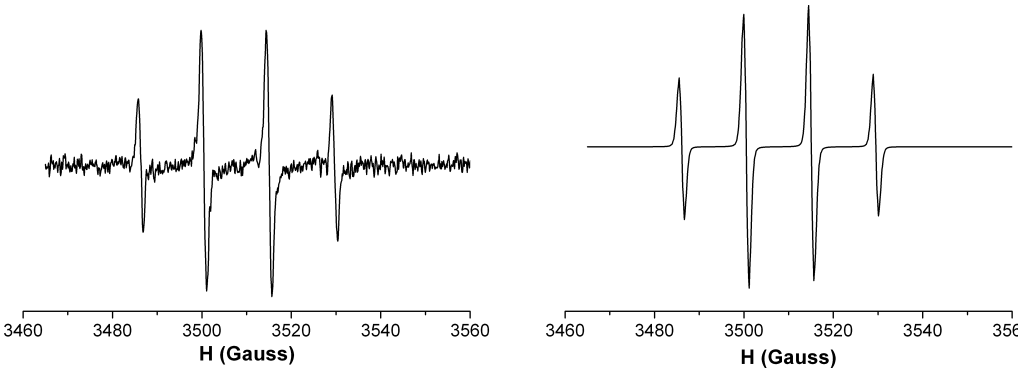

Fig. 7. Experimental (A) and simulated (B) CW ESR in band X spectra from spin trapping experiment with DMPO. Heterogeneous system: Co(II)-Poly(EGDE-MAA-2MI)/63 mM H_2O_2 with 200 U mL^{-1} SOD, in distilled water. The simulation and fits of the experimental spectrum allowed establishing the presence of DMPO/OH. It should be noted that the DMPO/OOH adduct is not present.

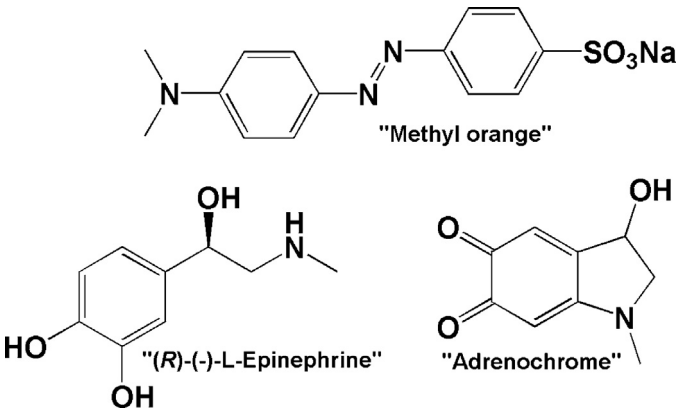

Scheme 3. Chemical structures of MO, epinephrine and adrenochrome.

This second possible mechanism predicts a molar fraction equal to 0.5 for each radical specie ($HO_2^{\bullet}$ and $OH^{\bullet}$), which is not consistent with our experimental evidence of a $O_2^{\bullet-}$ preponderance (Fig. 5B).

Agboola et al. presented spectroscopic evidence of the formation of cobalt intermediate species with catalytic activity ([(HOO)L-Co(III)]), when Co(II)-based homogeneous catalysts were oxidized by H_2O_2 [39,40]. In our heterogeneous system, both the [(HOO)L-Co(III)] intermediate and the radicals could eventually react with oxidizable compounds.

It must be taken into account that the surface of our catalyst is heterogeneous in terms of chemical composition. The different probable combinations of ligands on the coordination sphere of Co(II) in this heterogeneous catalyst would explain some heterogeneity in redox potentials of the active sites and thus the coexistence of both proposed mechanisms.

3.6. Decolorization of methyl orange

The oxidative activity of the free radicals from activated H_2O_2 was tested using the azo dye methyl orange (MO) as a model compound (Scheme 3). This dye was selected because of its low tendency to adsorb on the polyampholyte and its known susceptibility towards the advanced oxidation processes.

The experiments for removal of MO were carried out in distilled water and in 0.1 M Na_2SO_4 solution. Na_2SO_4 was used to minimize the dye adsorption on the catalyst, since this negatively-charged organic compound is electrostatically attracted by the positive sites on the polyampholyte surface. Phosphate, chloride and nitrate were discarded since each of them affected the efficiency of the overall process.

As a first approach, we studied the adsorption of MO on the catalyst.

The kinetic profiles of MO removal in the presence of Co(II)-poly(EGDE-MAA-2MI) and in the absence of H_2O_2 were compared for the two media (Supplementary content, Fig. A.7). The experimental data were fitted to the following empirical model:

$$[MO]_t = [MO]_\infty + [MO]_n \times e^{-k_n \times t} \quad (7)$$

where $[MO]_\infty$ is the amount of non-adsorbed dye, $[MO]_n$ is the amount of dye removed by adsorption, and k_n is the pseudo-first-order kinetic constant for the exponential decay of the dye concentration from the nth term of the equation. The parameters estimated for the different data sets are presented in Table 3.

In the absence of H_2O_2, MO was adsorbed on Co(II)-Poly(EGDE-MAA-2MI) from an initial dye concentration of 41 ± 1 μM, to an extent that depended on the composition of the medium. In distilled water, 52% of MO was removed in less than 1 h, and the rest was slowly uptaken by the matrix. The empirical kinetic model involves two terms describing the decrease in MO (Table 3).

Table 3
Parameters estimated for the changes in MO concentration due to adsorption on Co(II)-Poly(EGDE-MAA-2MI), from the empirical model presented in Eq. (7). The adsorption was tested in two different media (0.1 M Na_2SO_4 and distilled water), using 0.1000 g of the Co(II)-Poly(EGDE-MAA-2MI) complex in 100 mL of 41 ± 1 μM MO solution.

MO adsorption in 0.1 M Na_2SO_4		MO adsorption in water	
$[MO]_{ads}$ (μM)	2.51 S.D.: 0.10	$[MO]_{ads\,1}$ (μM)	22.59 S.D.: 0.38
k_{ads} (min^{-1})	0.246 S.D: 0.022	$k_{ads\,1}$ (min^{-1})	0.1011 S.D.: 0.0035
$[MO]_\infty$ (μM)	37.19 S.D.: 0.05	$[MO]_{ads\,2}$ (μM)	20.80 S.D.: 0.36
		$k_{ads\,2}$ (min^{-1})	0.0007 S.D.: 0.0002
R^2	0.9545	R^2	0.9982

The dissolved Na_2SO_4 clearly inhibited the adsorption of MO on the particles, since only 6.3% of the initial amount was withdrawn from the solution. The empirical model for this medium includes the amount of non-adsorbed dye (Table 3).

As a second approach, we explored the effect of the catalytic activation of H_2O_2 on the azo dye concentration (Fig. 8). The initial amount of H_2O_2 was set in 63 mM to optimize the efficiency in terms of degradation.

Without the polyampholyte, the homogeneous 0.35 mM Co(II)/63 mM H_2O_2 system oxidized less than 2% of the dye in 1 h. With these results we concluded that the amount of free radicals generated by free and soluble Co(II) species from the interaction with H_2O_2, was negligible.

The concentration of MO in the Co(II)-Poly(EGDE-MAA-2MI)/H_2O_2 system exhibited an exponential decay according to the empirical kinetic expression (8) in 0.1 M Na_2SO_4 and (9) distilled water. The parameters estimated are presented in Table 4

$$[MO]_t = [MO]_{ads} \times e^{-k_{ads} \times t} + [MO]_{deg} \times e^{-k_{deg} \times t} \quad (8)$$

$$[MO]_t = [MO]_{ads} \times e^{-k_{ads} \times t} + [MO]_{deg} \times e^{-k_{deg} \times t} + [MO]_\infty \quad (9)$$

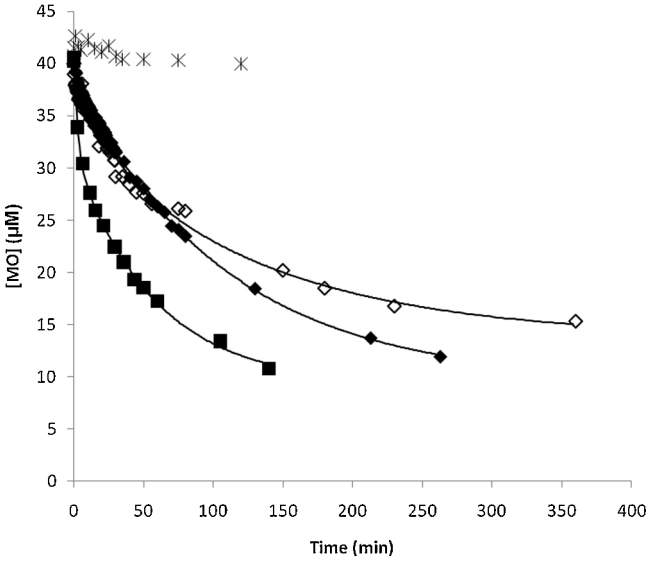

Fig. 8. MO concentration profile in the heterogeneous system, which consisted on 0.1000 g of the Co(II)-Poly(EGDE-MAA-2MI) complex in 100 mL of 41 ± 1 μM MO and 63 mM H_2O_2 solution. The reaction media were: 0.1 M Na_2SO_4 (♦) and distilled water (■). The catalyst was reloaded with Co(II) after the first cycle, and the experiment was repeated in 0.1 M Na_2SO_4 (◊). The homogeneous system was also tested with 41 μM MO, 0.35 mM Co(II), 63 mM H_2O_2 and 0.1 M Na_2SO_4 (*).

Table 4
Parameters estimated for the changes in MO concentration due to adsorption and degradation by the heterogeneous system, from the empirical models presented in Eqs. (8) and (9). The reaction was tested in two different media (0.1 M Na_2SO_4 and distilled water), using 0.1000 g of the Co(II)-Poly(EGDE-MAA-2MI) complex in 100 mL of 41 ± 1 μM MO and 63 mM H_2O_2 solution. The catalyst was tested on its first cycle of use, and on the second cycle with previous reloading of Co(II).

Condition	MO decoloration in water First catalytic cycle	MO decoloration in 0.1 M Na_2SO_4 First catalytic cycle	MO decoloration in 0.1 M Na_2SO_4 Second catalytic cycle; Co(II) reloaded
$[MO]_{ads}$ (μM)	9.09 S.D.: 0.56	1.96 S.D.: 0.14	5.5 S.D.: 3.9
k_{ads} (min^{-1})	0.343 S.D.: 0.047	0.558 S.D: 0.079	0.036 S.D.: 0.018
$[MO]_{deg}$ (μM)	21.96 S.D.: 0.51	29.09 S.D.: 0.20	19.3 S.D.: 2.9
k_{deg} (min^{-1})	0.0174 S.D.: 0.0014	0.0092 S.D.: 0.0010	0.0075 S.D.: 0.0024
$[MO]_{\infty}$ (μM)	9.33 S.D.: 0.63	9.50 S.D.: 0.22	13.7 S.D.: 1.4
R^2	0.9990	0.9991	0.9862

where $[MO]_{\infty}$ represents the free MO that decomposed with a very low kinetic constant since a complete removal was observed after 24 h of reaction; $[MO]_{ads}$ is the total amount of MO per litre of solution that would be removed by adsorption; and $[MO]_{deg}$ is the total amount of MO per litre of solution that would be removed by degradation. The pseudo-first-order kinetic constants (k) were assigned to each process.

The overall process of dye removal from the solution has a complex description involving surface adsorption on the catalyst and oxidative degradation. The degradation of MO is expected to be slower than the adsorption process which only involves mass transport and non-covalent bond formation.

Instead, the degradation process would involve mass transport of H_2O_2 to the catalyst and free radical formation on the catalytic surface in parallel with the eventual appearance of catalytically active cobalt intermediate species. The oxidative effect of the free radicals would require their mass transport to the bulk solution and the chemical oxidation reaction of the dye. Besides, the MO molecules should be transported to the particles surface to be oxidized by the cobalt intermediate species. In agreement with this, we assigned the term with the highest k to the adsorption process (Table 4 and Fig. 8).

From the tabulated values of the empirical parameters it can be observed that only 4.8% of MO was adsorbed on the catalyst in 0.1 M Na_2SO_4 (Table 4) and that 71.7% was degraded by means of radicals. Besides, the amount of adsorbed MO in 0.1 M Na_2SO_4 was close to the estimated in the absence of H_2O_2 (Tables 3 and 4).

On the other hand, only 54.4% of MO was degraded in distilled water, but the kinetic constant was 1.89 times higher than the k_{deg} estimated in the saline medium (Table 4).

Fig. 8 shows that near 70% of MO was removed from distilled water in 2 h. Instead, 70% of decolorization was achieved after 260 min in 0.1 M Na_2SO_4. Here, we considered both adsorption and degradation ways of decolorization.

It must be mentioned that in these experiments, the adsorbed MO was observed on the surface of the particles even when the solutions were almost decolorized. Then, we performed control experiments to evaluate the chemical stability of the adsorbed dye.

In the first control experiment, the MO was adsorbed on particles of the catalyst. In parallel, a H_2O_2 solution was put in contact with the solid particles of Co(II)-Poly(EGDE-MAA-2MI) during 10 min in order to activate the H_2O_2 and to get the maximal concentration of free radicals. Then, the MO-loaded Co(II)-poly(EGDE-MAA-2MI) was put in contact with activated H_2O_2. Here we observed a partial decolorization of the particles during the first 60 min of contact, and the complete absence of adsorbed MO after 8 h. When the control experiment was repeated without the previous step of H_2O_2 activation, the MO colour was preserved on the particles during the first 60 min but the decolorization was complete after 12 h. Evidently, the immobilized dye was also susceptible to the oxidative degradation, and the adsorbed MO would affect in some extent the kinetics of H_2O_2 activation.

The effect of the amount of catalyst on the decolorization rate was also studied. When we changed the *solution volume* (L) *to mass of catalyst* (g) ratio from 1 to 2.5 in distilled water, there was an increase of 33.4% in $[MO]_{deg}$ and a decrease of 85.6% in k_{deg}, compared with the corresponding parameters for a ratio equal to 1 (Supplementary content, Fig. A.8 and Table A.1). Besides, a lower H_2O_2 initial concentration significantly affected the $[MO]_{ads}$ (leading to higher amounts) and the k_{deg}, as expected (Supplementary content, Table A.1).

Regarding the degradation products, we observed that the UV–visible spectra of the treated extracts of MO exhibited absorption bands at 400 nm even when the solution was already decolorized (Supplementary content, Fig. A.9). This was consistent with the presence of aromatic products, indicating that the mineralization was not achieved [15–17].

The next experiments were conducted to put in evidence the main mechanism of MO degradation, the role of the solid matrix and the potential participation of cobalt intermediate species in the MO oxidative reaction.

First, the H_2O_2 solution was activated during 10 min with the solid particles of Co(II)-Poly(EGDE-MAA-2MI). Then, the suspension was filtered, the supernatant was mixed with concentrated MO solution, and the MO concentration was monitored as a function of time. The concentration of the dye exhibited a lag phase during the first 10 min, followed by a pseudo-first order exponential decay with a k_{deg} equal to $0.0089 \pm 0.0002\ min^{-1}$ (Fig. 9). This parameter coincided with the kinetic constant estimated for the degradation process ($0.0092 \pm 0.0010\ min^{-1}$) when the whole Co(II)-Poly(EGDE-MAA-2MI)/63 mM H_2O_2 heterogeneous system was used (Table 4). In this supernatant solution, the degradation of MO can be attributed exclusively to the oxidative action of the free radicals from the previously activated H_2O_2. The control experiment performed with MO and H_2O_2 in absence of the catalyst, showed no changes in the absorbance of the solution (Fig. 9).

Besides, we combined the independent results obtained from the MO adsorption on the catalyst and the results from the degradation of MO by action of the free radicals from the supernatant. The simulated profile arisen from this combination clearly coincided with the MO decolorization performed with the whole Co(II)-Poly(EGDE-MAA-2MI)/63 mM H_2O_2 heterogeneous system (Fig. 9).

In a second approach, we intended to evidence the formation of cobalt intermediate species and to study their role on MO degradation. This time, the solid particles of Co(II)-Poly(EGDE-MAA-2MI) were activated with H_2O_2 and put in contact with a MO solution; the resulting profile of dye concentration was consistent with the

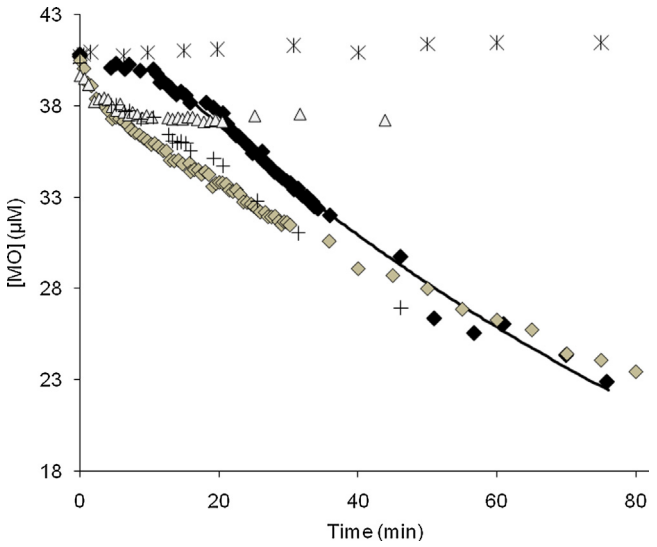

Fig. 9. MO concentration profile in 0.1 M Na_2SO_4 under different experimental conditions: with 63 mM H_2O_2 (◦); with Co(II)-Poly(EGDE-MAA-2MI) (▲); with Co(II)-Poly(EGDE-MAA-2MI)/63 mM H_2O_2 (♦); with the supernatant of Co(II)-Poly(EGDE-MAA-2MI)/63 mM H_2O_2 (contact time with catalyst: 10 min) (♦); the sum of the individual effects of MO adsorption and degradation by supernatant (+).

decolorization by adsorption on the solid (Supplementary content, Fig. A.10).

Then, the activation of the solid with H_2O_2 was repeated twice, and the activated catalyst was put in contact with the same MO solution after each activation cycle, resulting in a small decrease of MO concentration when the equilibrium was reached. In this case, the MO adsorbed on the first contact would have been degraded during the second activation cycle, regenerating some binding sites (Supplementary content, Fig. A.10). If any cobalt intermediate species were formed during the activation of the catalyst, there was not enough evidence of their direct catalytic activity on MO oxidative degradation.

Based on this experimental evidence, we conclude that the main mechanism of MO degradation would involve the oxidative action of the free radicals present in the bulk solution. The direct contribution of a hypothetical cobalt intermediate specie from the particles on the dye oxidation would be minimal. The MO adsorbed on the catalyst particles would not be degraded by the catalytic sites of the surface; instead, it would suffer the oxidative attack of the $O_2^{\bullet -}$ from the solution, decolorization with a slower kinetics than the solubilized MO.

3.7. Catalyst reuse and stability

The Co(II)-Poly(EGDE-MAA-2MI) complex was recovered and re-used in three cycles of reaction in order to confirm that this material is not a reagent and to demonstrate the catalytic activity of the solid.

Both adsorption and degradation of MO took place during the first cycle of 30 min in 0.1 M Na_2SO_4, and only degradation was expected in the following cycles. In the third cycle, only 27% of MO was degraded and the k_{deg} was the 82% of the value obtained in the first cycle (Supplementary content, Fig. A.11).

Based on these results, we considered the cobalt leaking as a possible cause of the loss of efficiency in successive cycles.

In our system, we found a release of 88.4 μg of Co(II) in 10.0 mL of reaction at equilibrium after the first catalytic cycle, which represents 28.8% of the total Co(II) in the system. It must be pointed out that this exhausted solution recovered from this first catalytic cycle did not exhibit catalytic activity upon the addition of more MO and H_2O_2, in the absence of the catalyst. On the other hand, the amount of Co(II) leached was not dependent of the composition of the medium.

For the second and third catalytic cycle, we detected 19.4 μg (6.32%) and 0.92 μg (3.00%), respectively. This means that the 30% of the adsorbed Co(II) interacts weakly with the polyampholyte, and the other fraction is mostly retained by the matrix in successive cycles of use. Here, the H_2O_2 acting as ligand of Co(II) in the activation reaction, would compete with the weaker ligand groups of the polymer (such as $-COO^-$) for the coordination of the cation, leading to some extent of cobalt release from the heterogeneous catalyst. This assumption is supported on the fact that the polyelectrolyte named poly(EGDE-MAA) has very low capacity for Cu(II) and Co(II), requiring high concentration levels of the cation to form the respective coordination complexes [10,11].

Cobalt salts are frequently used in catalysis of organic chemical reactions, as well as in painting pigments, B12 vitamin manufacturing, and as foam stabilizer in beer, among other applications. Regarding the environmental concern, cobalt ions have both beneficial and harmful effects on health [41–43]. In order to overcome the cobalt leak, we recommend the use of the non-complexed polyampholyte (Poly(EGDE-MAA-2MI) as an adsorbent for the dissolved ions released from the catalyst after the treatment with H_2O_2. The loading capacity of this resin for Co(II) ions was already estimated in 30.7 mg g^{-1} (Table 1).

In order to explore the regeneration of the catalyst used for the first catalytic cycle, it was recovered, reloaded with Co(II) and tested again on the activation of H_2O_2 for decolorization of MO solutions (Fig. 8). Here we found that the k_{deg} did not change significantly when compared with the first catalytic cycle, indicating that the efficiency on H_2O_2 activation was recovered with Co(II) reloading (Table 4). On the other hand, the k_{ads} decreased a 93.5% meanwhile $[MO]_{ads}$ did not suffer a significant variation, indicating that some reversible surface changes resulted from the overall treatment. The MO molecules, which bear negative electric charge from the sulfonate group, would interact with the free 2MI residues at the time that these groups become protonated due to the release of H^+ from H_2O_2 activation.

From these result we also concluded that the catalyst needs to be reloaded with Co(II) ions between cycles in order to get the most efficient performance. At this moment, our working group is focussing the research towards the synthesis of stronger ligands (alternative to 2MI) to be incorporated to the polyampholyte, in order to overcome the cation leak.

3.8. Oxidation of epinephrine

The catalytic activation of H_2O_2 was also assessed with epinephrine as a model compound of pharmaceuticals. Epinephrine is a catecholamine which can be oxidized by superoxide to the strongly absorbing product adrenochrome (catecholamine *o*-quinone; Scheme 3) [19]. Its presence is detected in solution by a pink colour, which then turns brown upon polymerization.

Fig. 10 presents the results of the epinephrine conversion in the presence of H_2O_2 and Co(II)-Poly(EGDE-MAA-2MI). About 80% of conversion was reached in less than 6 min, with a pseudo-first-order kinetic constant of 0.397 ± 0.025 min^{-1}.

In the absence of catalyst, the oxidation of epinephrine by H_2O_2 was practically negligible.

A control experiment performed with epinephrine and Co(II)-Poly(EGDE-MAA-2MI) in the absence of H_2O_2 exhibited some extent of catecholamine oxidation, being less efficient than the oxidation by H_2O_2. Then, the control experiment was repeated, this time with previous and continuous bubbling of argon to displace the dissolved O_2 and to saturate the atmosphere with the inert gas. Here, the amount of adrenochrome released was negligible

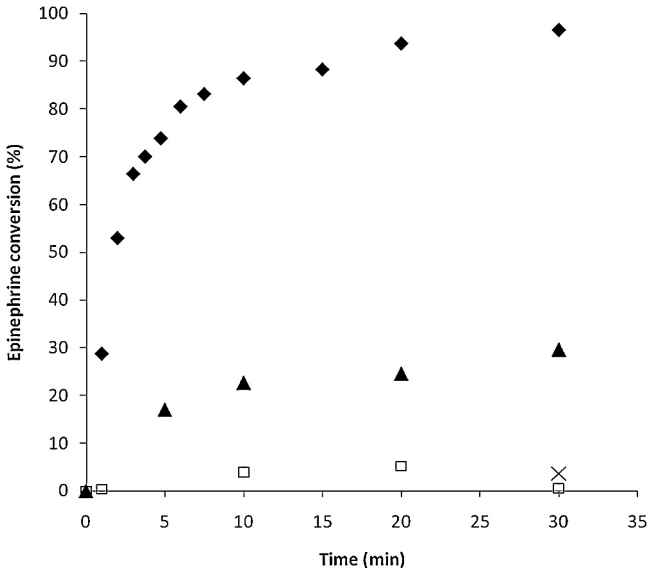

Fig. 10. Percent of epinephrine conversion to adrenochrome in 0.1 M Na_2SO_4 solution: in the presence of Co(II)-Poly(EGDE-MAA-2MI) (▲), in the presence of Co(II)-Poly(EGDE-MAA-2MI) with argon bubbling (×), in the presence of Co(II)-Poly(EGDE-MAA-2MI) and 46 mM H_2O_2 (♦), and in the presence of 46 mM H_2O_2 (□).

(Fig. 10), indicating that the oxidation of epinephrine could also be achieved with atmospheric O_2, when it was activated in some way by Co(II)-Poly(EGDE-MAA-2MI).

4. Conclusions

A chemically stable coordination complex was prepared with Co(II) and the polyampholyte Poly(EGDE-MAA-2MI). The interaction between the polymer and Co(II) was well characterized by solid-state NMR spectroscopy.

The catalytic activity of this material on H_2O_2 activation could be deeply studied by ESR. We could propose a mechanism of reaction which involves the simultaneous production of superoxide radical, dioxygen, protons and water. This mechanism was different from the H_2O_2 activation by the Cu(II)-Poly(EGDE-MAA-2MI) complex described in a previous article.

This complex combined effectiveness in H_2O_2 activation, ease of recovery and aptitude for regeneration.

The high loading capacity of the polyampholyte for ionic species may lead to the adsorption of solutes, which would affect the catalytic efficiency in the oxidative treatment of complex samples. This drawback can be conveniently overcome by the addition (if not yet present) of a certain amount of inorganic salts such as sodium or potassium sulfate.

The superoxide radicals are considered less reactive than hydroxyl species, leading to an oxidative treatment of mild strength.

In the treatment of MO, the mineralization of the organic compound was not achieved, according with the spectral evidence. We must recall that MO solutions have been found to be toxic for some model plants and bacteria, which would prevent the choice of biological methods as the starting way of decolorization of wastewater. Then, our "green and mild" oxidative treatment could be useful to initiate the degradation (until exhaustion of H_2O_2), which could eventually be completed by microorganisms that use small organic compounds as carbon and/or nitrogen source.

Superoxide radicals can also be useful to accelerate some degradation processes in which the substrate has a low reduction potential. Besides, the amount of oxidant necessary to produce an effective concentration of free radicals can also be minimized with our method.

In this same context, the method can be useful to obtain partially oxidized industrial products like adrenochrome from epinephrine (a precursor of haemostatic drugs such as carbazochrome), which is usually synthesized with Ag_2O as oxidant [44,45]. Here, Ag^+ could be replaced by an oxidant of lower environmental impact.

As a summary, the applicability of this cobalt-based polymeric catalyst combined with H_2O_2 is acceptable in terms of both performance and low environmental impact.

Acknowledgements

The authors thank the financial support from University of Buenos Aires (UBACyT 10-12/237 and 11-14/915), CONICET (CONICET 2010-2012/PIP 076), ANPCyT (BID 1728/PICT 01778 and BID Bicentenario/PICT 1957). L.V. Lombardo Lupano thanks the CONICET for her doctoral fellowship and Dr. J.M. Lázaro Martínez thanks the CONICET for his post-doctoral fellowship. The authors thank Dr. Victor Busto (Department of Microbiology, Immunology and Biotechnology, Faculty of Pharmacy and Biochemistry, University of Buenos Aires) for the measurements of partial pressure of dioxygen.

Appendix A. Supplementary data

Supplementary data associated with this article can be found, in the online version, at http://dx.doi.org/10.1016/j.apcata.2013.08.002.

References

[1] D.E. Richardson, H.R. Yao, K.M. Frank, D. Bennett, J. Am. Chem. Soc. 122 (2000) 1729–1739.
[2] C.W. Jones (Ed.), Applications of Hydrogen Peroxide and Derivatives, RSC, London, 1999.
[3] W. Hess, J. Treutwein, G. Hilt, Synthesis (2008) 3537–3562.
[4] E.K. Beloglazkina, A.G. Majouga, R.B. Romashkina, N.V. Zyk, Tetrahedron Lett. 47 (2006) 2957–2959.
[5] D. Gao, Q. Gao, Catal. Commun. 8 (2007) 681–685.
[6] Y. Zhang, Z. Li, W. Sun, C. Xia, Catal. Commun. 10 (2008) 237–242.
[7] B. Tamami, S. Ghasemi, Appl. Catal. A 393 (2011) 242–250.
[8] W. Lu, W. Chen, N. Li, M. Xu, Y. Yao, Appl. Catal. B 87 (2009) 146–151.
[9] M.F. Leal Denis, R.R. Carballo, A.J. Spiaggi, P.C. Dabas, V. Campo Dall' Orto, J.M. Lázaro Martínez, G.Y. Buldain, React. Funct. Polym. 68 (2008) 169–181.
[10] J.M. Lázaro Martínez, M.F. Leal Denis, V. Campo Dall' Orto, G.Y. Buldain, Eur. Polym. J. 44 (2008) 392–407.
[11] J.M. Lázaro Martínez, A.K. Chattah, G.A. Monti, M.F. Leal Denis, G.Y. Buldain, V. Campo Dall' Orto, Polymer 49 (2008) 5482–5489.
[12] J.M. Lázaro Martínez, A.K. Chattah, R.M. Torres Sánchez, G.Y. Buldain, V. Campo Dall' Orto, Polymer 53 (2012) 1288–1297.
[13] J.M. Lázaro Martínez, M.F. Leal Denis, L.L. Piehl, E. Rubín de Celis, G.Y. Buldain, V. Campo Dall' Orto, Appl. Catal. B 82 (2008) 273–283.
[14] Methyl Orange Material Safety Data Sheet, Santa Cruz Biotechnology, Inc., 2007.
[15] F. Chen, Y. Xie, J. He, J. Zhao, J. Photochem. Photobiol. A: Chem. 138 (2001) 139–146.
[16] C. Baiocchi, M.C. Brussino, E. Pramauro, A. Bianco Prevot, L. Palmisano, G. Marcí, Int. J. Mass Spectrom. 214 (2002) 247–256.
[17] Y. He, F. Grieser, M. Ashokkumar, Ultrason. Sonochem. 18 (2011) 974–980.
[18] G.K. Parshetti, A.A. Telke, D.C. Kalyani, S.P. Govindwar, J. Hazard. Mater. 176 (2010) 503–509.
[19] R. Alhasan, D. Njus, Anal. Biochem. 381 (2008) 142–147.
[20] Z. Tao, G. Wang, J. Goodisman, T. Asefa, Langmuir 25 (17) (2009) 10183–10188.
[21] B.M. Fung, A.K. Khitrin, K. Ermolaev, J. Magn. Reson. 142 (2000) 97–101.
[22] A.M. El-Brashy, M. El-Sayed Metwally, F.A. El-Sepai, J. Chin. Chem. Soc. 52 (2005) 77–84.
[23] M. Hadi, M.R. Samarghandi, G. McKay, Chem. Eng. J. 160 (2010) 408–416.
[24] K. Burnham, D. Anderson, K. Huyvaert, Behav. Ecol. Sociobiol. 65 (2011) 23–35.
[25] G.J. Copello, L.E. Diaz, V. Campo Dall' Orto, J. Hazard. Mater. 217–218 (2012) 374–381.
[26] M.B. Ettinger, C.C. Ruchhoft, R.J. Lishka, Anal. Chem. 23 (12) (1951) 1783–1788.
[27] L.R. Denaday, M.V. Miranda, R.M. Torres Sánchez, J.M. Lázaro Martínez, L.V. Lombardo Lupano, V. Campo Dall' Orto, Biochem. Eng. J. 58–59 (2011) 57–68.
[28] D.D. Do, Adsorption Analysis: Equilibria and Kinetics, vol. 2, Imperial College Press, London, 1998.

[29] F. Haghseresht, G.Q. Lu, Energy Fuel 12 (1998) 1100–1107.
[30] C. Aharoni, D.L. Sparks, in: D.L. Sparks, D.L. Suarez (Eds.), Rates of Soil Chemical Processes, Soil Science Society of America, Madison, WI, 1991, pp. 1–18.
[31] C.-T. Hsieh, H. Teng, J. Chem. Technol. Biotechnol. 75 (2000) 1066–1072.
[32] J.P. Hobson, J. Phys. Chem. 73 (1969) 2720–2727.
[33] I.H. Gübbük, R. Güp, M. Ersöz, J. Colloid Interface Sci. 320 (2008) 376–382.
[34] I. Bertini, P. Turano, A.J. Vila, Chem. Rev. 93 (1993) 2833–2932.
[35] P.L. Zamora, F.A. Villamena, J. Phys. Chem. A 116 (2012) 7210–7218.
[36] S.-X. Liang, L.-X. Zhao, B.-T. Zhang, J.-M. Lin, J. Phys. Chem. A 112 (2008) 618–623.
[37] G.R. Buettner, Free Radical Biol. Med. 3 (1987) 259–303.
[38] J.M. Lázaro Martínez, E. Rodríguez-Castellón, R.M. Torres Sánchez, L.R. Denaday, G.Y. Buldain, V. Campo Dall' Orto, J. Mol. Catal. A: Chem. 339 (2011) 43–51.
[39] C. Shen, S. Song, L. Zang, X. Kang, Y. Wen, W. Liu, L. Fu, J. Hazard. Mater. 177 (2010) 560–566.
[40] B. Agboola, K.I. Ozoemena, T. Nyokong, J. Mol. Catal. A: Chem. 227 (2005) 209–216.
[41] S. Rengaraj, S.-H. Moon, Water Res. 36 (2002) 1783–1793.
[42] M.F. Abdel-Sabour, J. Environ. Sci. 15 (3) (2003) 388–395.
[43] D.S. Pines, D.A. Reckhow, Environ. Sci. Technol. 36 (2002) 4046–4051.
[44] MacCarthy, Chim. Ind. Paris 55 (1946) 435.
[45] M. Verstraete, Haemostatic Drugs, Springer, Netherlands, The Hague, 1977, pp. 59–66.